

Article

Visualization of Annular Gap Junction Vesicle Processing: The Interplay between Annular Gap Junctions and Mitochondria

Cheryl L. Bell ¹, Teresa I. Shakespeare ² and Sandra A. Murray ^{1,*}

¹ Department of Cell Biology, School of Medicine, University of Pittsburgh, Pittsburgh, PA 15261, USA; clb206@pitt.edu (C.L.B.); smurray@pitt.edu (S.A.M.)

² Department of Biology, Savannah State University, Savannah, GA 31404, USA; shakespearet@fvsu.edu (T.I.S.)

* Correspondence: smurray@pitt.edu; Tel.: +01-412-648-9566

Abstract: It is becoming clear that in addition to gap junctions, playing a role in cell-cell communication, gap junction proteins, connexins, located in cytoplasmic compartments may have other important functions. Mitochondrial connexin 43 (Cx43) is increased after ischemic preconditioning and has been suggested to play a protective role in the heart. How Cx43 traffics to the mitochondria and the interactions of mitochondria with other Cx43-containing structures are unknown. In this study, immunocytochemical, super-resolution and transmission electron microscopy were used to detect cytoplasmic Cx43-containing structure and to demonstrate their interactions with other cytoplasmic organelles. The most prominent cytoplasmic Cx43-containing structures, annular gap junctions, were demonstrated to form intimate associations with lysosomes as well as with mitochondria. Surprisingly, the frequency of associations between mitochondria and annular gap junctions was greater than that between lysosomes and annular gap junctions. The benefits of annular gap junction/mitochondrial associations are not known. However, it is tempting to suggest that the contact between annular gap junction vesicles and mitochondria facilitates Cx43 deliver to the mitochondria. Furthermore, it points to the need for investigating trafficking of Cx43 to cytoplasmic compartments and annular gap junction as more than only a vesicle destined for degradation.

Keywords: Gap Junction; Connexin; Annular Gap Junction Vesicle; Mitochondria; Lysosome

1. Introduction

Gap junction channels play a pivotal role in a vast number of physiological events by providing channels for the intercellular communication of regulatory molecules between cells[1]. Gap junction channels are composed of gap junction proteins, termed connexin[2]. All of the members of the multigene connexin family have a similar topology and the sequences of several connexin gap junction proteins have been determined[3,4]. Connexin 43 (Cx43) gap junction protein, the most ubiquitously expressed connexin, is thought to be synthesized in the endoplasmic reticulum, oligomerized into a hemichannel in the Golgi[5] and then transported to the cell surface in secretory vesicles. On the cell surface, hemichannels from apposing cells align (dock) to form channels[6]. Gap junction channels then aggregate to form gap junction plaques[1]. These gap junction plaques are composed of thousands of channels[6]

and plaque size is determined by the number of hemichannels that are delivered to the membrane in secretory vesicles and aggregated on the surface to form these plaques[6]

Gap junction plaques are removed from the cell surface by an internalization event[7,8]. The disassembly and removal of gap junction plaques from the plasma membrane involve a clathrin/dynamin dependent unique internalization process[9-12] in which the gap junction plaque that connects two adjacent cells is internalized into the cytoplasm of one of the cells to form an annular gap junction[13-15]. These annular gap junctions were first identified with transmission electron microscopy (TEM) and were distinguished from other organelles by the presence of a double-membrane (pentalaminar membrane) and a central lumen[7,13-18]. Annular gap junctions (also called connexosomes) have now been demonstrated with live cell imaging techniques to form from internalization at central regions of the gap junction plaque[19-22] or internalization of the entire gap junction plaque[23].

The central dogma has been that the gap junction proteins (connexins) in these annular gap junctions are degraded, and thus the internalization process is only a method of eliminating old connexins[7,14,24]. However, data from our laboratory and that of others has demonstrated that connexins, specifically annular gap junction vesicle connexin 43 (Cx43), recycle back to the cell surface to form functional gap junctions[25,26]. While the aggregation of gap junction channels into plaques and channel gating have been extensively studied[19,27,28], mechanisms involved in the processing of annular gap junction vesicles have only recently gained attention. However, it is clear that, the rates of gap junction plaque disassembly as well as assembly are critical to gap junction function in cell-cell communication and cell-cell adhesion[29,30]. Changes in gap junction location and connexin trafficking and internalization is thought to play several pivotal physiological roles during embryonic development [31,32], mitosis[26], wound healing[33], and cell migration and these changes are thought to facilitate tumor growth and metastasis as well as cardiac muscle changes during ischemia[34-36]. Other than considering secretory vesicles as the mechanism of Cx43 delivery, alternative Cx43 cytoplasmic delivery sources have received little attention. It has been demonstrated however that there is Cx43 on mitochondrial membranes, and this mitochondrial Cx43 was shown to be essential for ischemic preconditioning[34]. Further, N-terminal truncated isoforms of Cx43 have been demonstrated to play a role in mitochondrial movement to the cell periphery and in maintaining the mitochondrial network integrity during oxidative stress in cardiomyocytes and cold stress in adipocytes [37-39]. The method of Cx43 delivery to the mitochondria is not understood. Furthermore, the possible pathophysiological role of Cx43 within cytoplasmic compartments or associations between these compartments is not known. Understanding Cx43 trafficking, fate and the translocation to Cx43-containing organelles is essential to an understanding of a host of normal and pathological events.

In this study, we demonstrated cytoplasmic Cx43-containing structures and evaluated their organelle interactions. We found that the most abundant Cx43-containing structures, annular gap junction vesicles, associated more frequently with mitochondria than with lysosomes. These findings are consistent with the possibility that some of the Cx43 present in annular gap junctions may be utilized by mitochondria rather than being only degraded.

2. Results

2.1. Characterization of Cx43 Containing Gap Junctions Structure Behavior

A human adrenal tumor cell line (SW-13) that expresses Cx43 gap junction protein was used to analyze cytoplasmic Cx43-containing structures, particularly that of annular gap junction vesicles, which are the most prominent Cx43-containing organelle in the cytoplasm (Figure 1A). This cell line forms relatively large gap junctions which are spontaneously and frequently internalized to form annular gap junction vesicles, which is particularly advantageous for the study aspects of Cx43 trafficking. With immunocytochemistry and live cell imaging techniques, gap junction plaques could be seen at the cell

surface between contacting cells (Figures 1A-B, and 2). Puncta indicative of annular gap junction vesicles could be easily seen within the cytoplasm (Figures 1 and 2). In addition, secretory vesicles that deliver new Cx43 to the plasma membrane could be detected at the light level of resolution, but they were more easily discerned with super-resolution microscopy (Figure 1C). Secretory and annular gap junction vesicles both appeared as puncta at the light microscopic level of resolution and are distinguished mainly by the differences in their sizes. Annular gap junction vesicles ($\geq 0.5\mu\text{m}$) have been demonstrated to be larger than the secretory vesicles ($\leq 150\text{nm}$) [19,40]. With transmission electron microscopy the pentalaminar membrane of annular gap junction vesicles, which is a typical characteristic of the gap junction plaque membrane, can be used to distinguish this vesicle from other cytoplasmic organelles. (Figure 1D-E).

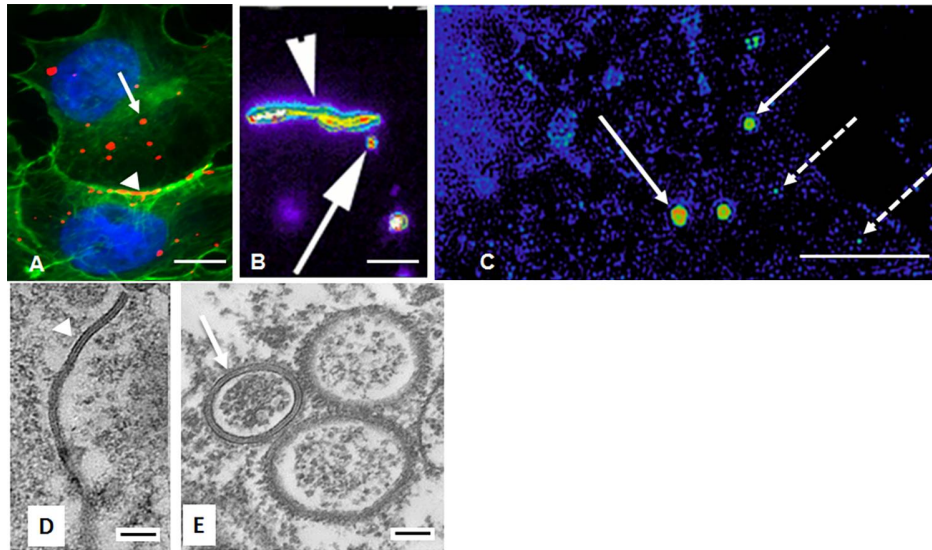


Figure 1. Localization of gap junction plaques and annular gap junction vesicles. A) Immunocytochemistry of Cx43 (red) and cortical actin (green). Cortical actin (green) staining was used to define the boundaries of the cell and to aid in distinguishing intracellular annular gap junction puncta (red, arrow) from surface gap junction plaques (red, arrowhead). (B) Pseudo-colored image of Cx43-GFP from a time lapse frame demonstrating gap junction plaques (arrowhead) and annular gap junction vesicles (arrow). (C) Super-resolution microscopy demonstrating annular gap junction (arrow) and secretory vesicles (broken arrow). (D, E) TEM demonstrating the typical pentalaminar membrane of the gap junction plaque (arrowhead in E) and annular gap junction vesicle (arrow in E). Scale Bars= (A-B):10 μm, (C): 5 μm, (D-E): 100 nm

In addition to annular gap junctions and secretory vesicles, ultrastructural analysis revealed occasional membrane fragments of various sizes, atypical aggregates of gap junction membrane as well as bizarre looking structures in the cytoplasm which were composed of gap junction membranes (Figure 3). The fragments were identified by the typical gap junction membrane while the more bizarre structures were further confirmed as composed of Cx43 with immuno-electron microscopy (Figure 3D). Given the recent suggestion that Cx43 in annular gap junctions could have fates other than only degradation, we did a detailed analysis of annular gap junction processing and their associations with other organelles.

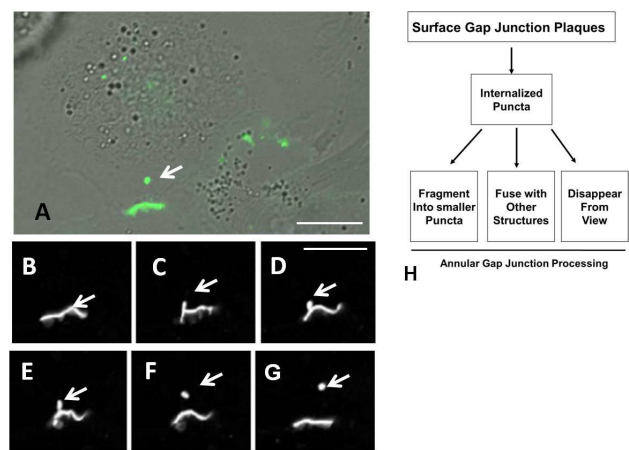


Figure 2. Time lapse imaging of cells expressing Cx43-GFP. (A) DIC image of cell population seen in the time lapse images collected at 1 minute intervals in B-G. The gap junction plaque between two cells is evident as well as the cytoplasmic annular gap junction (arrow in A). (B-G) Time lapse montage (1 minute intervals) demonstrating the formation and release of the annular gap junction vesicle (arrows) into the cytoplasm of one of the two contacting cells. (H) Flow chart summary of annular gap junction formation and behavior. Scale Bars A-G:10µm

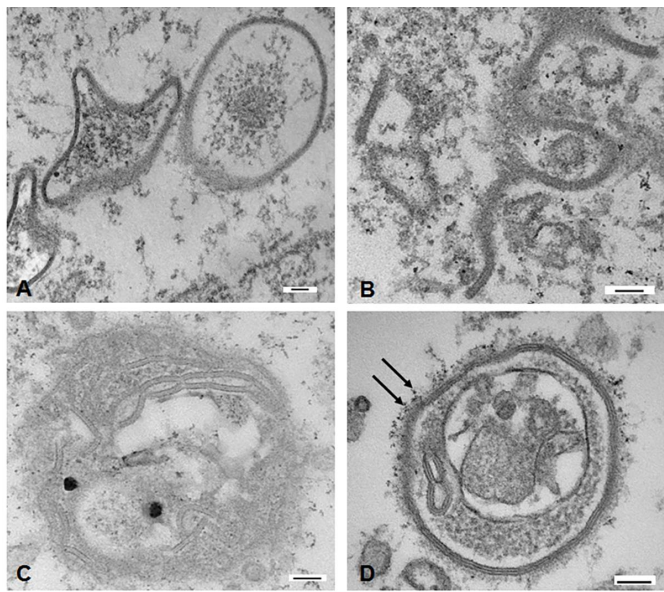


Figure 3. TEM of cytoplasmic gap junction structures. (A) Two star shaped annular gap junctions seen next to a typical annular gap junction vesicle. (B) Fragmented gap junction membrane. Note the pentalaminar membrane. (C) Aggregates of gap junction membrane arranged in an annular shape. (D) Bizarre annular gap junction with annular structure and other unknown material within the lumen. Immuno-electron microscopic Cx-43 Q-dots (arrows) can be seen labeling the annular gap junction membrane. Scale Bars= (A-D): 100 nm

2.1.1. Live Cell Imaging of Gap Junction Plaque Endoexocytosis

Since at the light microscopic level the distinguishing pentalaminar membrane was not visible, positive identification of annular gap junctions in these live cell imaging studies was made by monitoring them, following observations of their internalization from gap junction plaques. Annular gap junction vesicles were observed to form both as a result of internalization of portions of gap junction plaques or entire gap junction plaques. In both cases the annular gap junction vesicle was released into one of two contacting cells (Figure 2). The internalization occurred rapidly if only a portion of the central area of the gap junction plaque was internalized, while internalization of the entire gap junction was a much slower process and resulted in larger annular gap junction vesicle being released into the cytoplasm. As summarized in figure 2H, over the 26-hour monitoring period, 93 annular gap junctions from four different movies were observed to either (a) remain relatively stationary within the cytoplasm, (b) fragment to form smaller puncta, (c) join with cytoplasmic organelles, (d) disappear from view or (e) move toward and appear to associate with the cell surface gap junction plaques.

Annular gap junctions that were observed to join with other cytoplasmic organelles, remained with these organelles throughout the monitoring period. These results prompted us to determine the identity of structures that associated with the annular gap junction vesicles.

2.2. Annular Gap Junction Fusion with Other Organelles

Annular gap junctions were observed With immunocytochemical localization techniques, annular gap junction vesicles were found to associate with two different organelles, lysosomes (Figure 4) as expected, and mitochondria (Figures 5,6). The details of these interactions were analyzed.

2.2.1. Analysis of Lysosomes/ Annular Gap Junction Associations

Lysosomes, detected with a lysosomal marker, Lamp 1, were shown to colocalize with annular gap junctions in cells expressing endogenous Cx43 (Figure 4A) as well as transfected to express Cx43-GFP (data not shown). An analysis of cytoplasmic puncta indicated that 8.3 ± 3.6 % of the endogenous Cx43 was colocalized with lysosomes. A higher percentage of the Cx43-GFP was found colocalized with the lysosome marker. We believe the higher localization with Cx43-GFP was due to increased aggregation of non-specific staining within the cytoplasm of transfected cells.

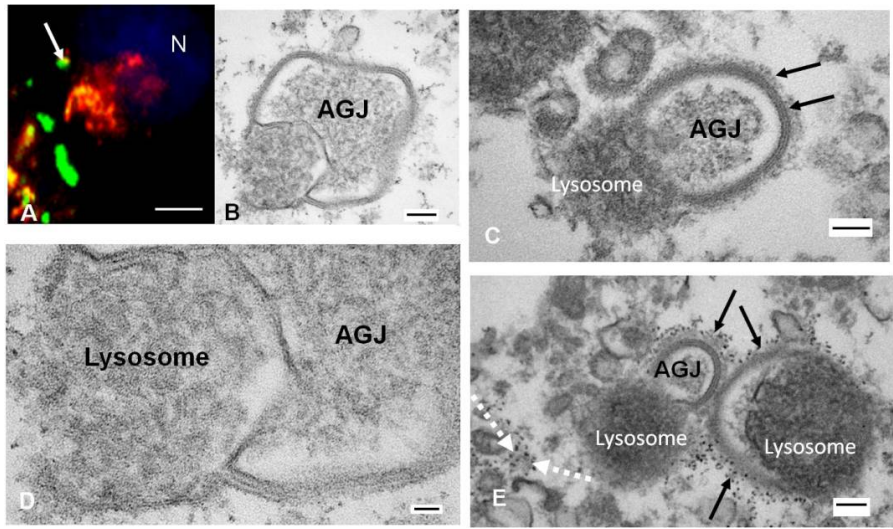


Figure 4. Localization of annular gap junction vesicles and Lysosomes (A) Immunocytochemical localization of Cx43 (green) and lysosomes detected with LAMP1 (red). The colocalization (yellow) of an annular gap junction vesicle and lysosome can be seen (arrow). (B-E) The intimate contact between annular gap junction (AGJ) and lysosomes is shown. In B and D the outer membrane of the annular gap junction can be seen to be continuous with that of the lysosomal membrane. Clathrin, identified by bristle coat (arrow, C) or quantum dot label (black arrows, E) can be seen associated with annular gap junction vesicles which are fused with lysosomes. Typical clathrin coated vesicles also can be seen decorated with clathrin Q dots (dashed white arrows). N= Nucleus; Scale Bars= (A): 10 μ m, (B, C, E): 100 nm, (D): 20 nm

A pitfall of interpreting colocalization data is that at the light microscopic level structures that are separated by as much as 200nm can still appear to be colocalized. Further, the capacity to distinguish and analyze the morphology of the organelles is limited by the resolution of images collected with light microscopy. To better resolve the morphology and to positively identify structures as well as demonstrate associations, transmission electron microscopic techniques were used.

The annular gap junction vesicle's pentalaminar membrane is highly distinctive when imaged by transmission electron microscopy [TEM] (Figures 1D&E, 4-6). Regardless of its shape or location in the cell this organelle can be identified. Taking advantage of the morphological characteristic of the annular gap

junction membrane and of other cytoplasmic organelles seen with TEM, we analyzed the association of organelles with gap junction structures.

Annular gap junctional vesicles were observed to interact with lysosomes and appeared to be in different stages of degradation (Figures 4B-E). In annular gap junctional profiles that appeared to be undergoing degradation the inner and outer annular gap junction membranes were separated from one another and the outer membrane was continuous with the lysosomal membrane (Figure 4B&C). Clathrin was found associated with the annular gap junction, even at the point that they were fused with lysosomes (Figure 4C&E). With ultrastructural analysis the number of lysosomal/annular vesicle associations could be quantitated in detail. Based on the analysis of 549 annular gap junction vesicles, we demonstrated that 2.6 % ± 0.6 were fused with lysosomes.

2.2.2. Mitochondria

In addition to colocalization with lysosomes, annular gap junctions were revealed with immunocytochemistry and super-resolution microscopy to colocalize with mitochondria (Figure 5). While with immunocytochemistry the size of the puncta was used to identify a structure as an annular gap junction, with super-resolution microscopy the annular gap junction lumen is evident (Figure 5B). With both techniques annular gap junctions were demonstrated to colocalize with mitochondria. In figure 5B, colocalization of mitochondria detected with antibody to TOM (red) could be seen with more than one annular gap junction vesicle detected with Cx43 gap junction antigen (green). Images were captured with stimulated emission depletion (STED) super-resolution microscopy.

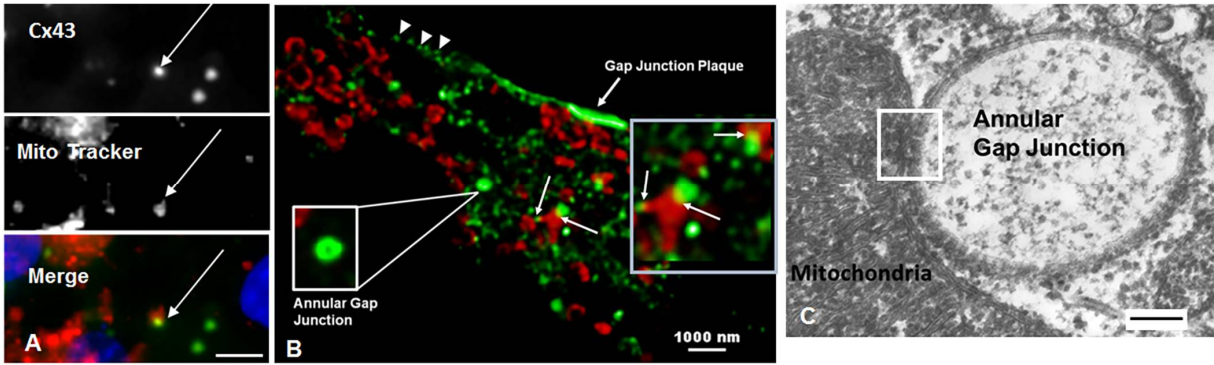


Figure 5. Mitochondria associate with annular gap junctions. (A, B) Immunocytochemical analysis of mitochondria (red) and Cx43 gap junction antigen (green). The mitochondria were detected with Mitotracker (red) in A and with antibody to TOM (red) in b. (C) The intimate association between the mitochondria and annular gap junction (white box) seen with TEM. Scale bars= (A): 10 μ m, (B): 1000 nm, (C) 100 nm

To visualize the fine structure morphology at the sites of physical association between the mitochondria and annular gap junctions, transmission electron microscopy (TEM) imaging was used (Figures 5, 6). Mitochondria were observed to associate and to follow the contour of annular gap junction membranes (Figures 5, 6). In some cases, actual contact sites between the outer membrane of the annular gap junction vesicles and mitochondria were evident (Figure 6). Ultrastructural analysis of 549 images of

annular gap junctions revealed that (5.2 % ± 1.1) associated with mitochondria. This percentage exceeded the percentage of annular gap junction vesicles that were found to associate with lysosomes (2.6 % ± 0.6).

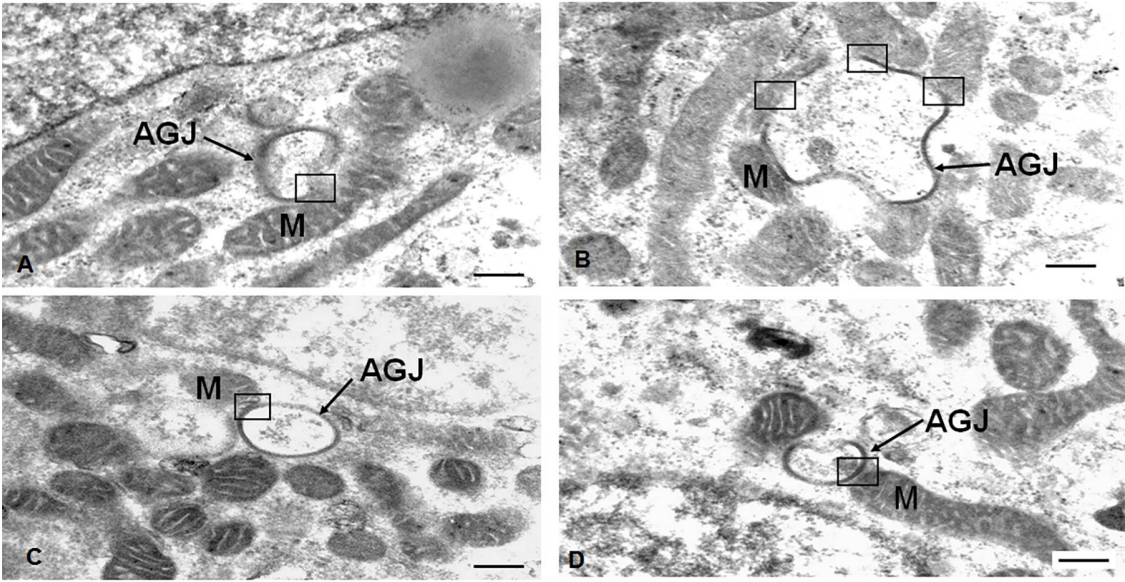


Figure 6. Transmission electron microscopy of mitochondria closely associated with annular gap junctions. A-B) Areas of contact between annular gap junctions (AGJ) and mitochondria (M) are indicated within the black boxes. Scale Bars: 500 nm

3. Discussion

In this study, we documented the presence of cytoplasmic Cx43-containing structures and we analyzed the details and frequency of interactions of mitochondria and lysosomes with annular gap junction vesicles. We found that the interactions between annular gap junctions and mitochondria were seen more frequently than between annular gap junctions and lysosomes. The behavior of the puncta believed to be annular gap junctions were analyzed with live cell imaging and it was determined that these structures could either: 1) undergo fission, 2) fuse with other organelles, 3) disappear from view, or appear to recycle back to the surface. In this study, to address the concern that in our live cell imaging studies GFP tag may either interfere with or alter organelle interactions with Cx43-containing structure, or that the Cx43 puncta were not positively identified as annular gap junction vesicles, we took advantage of TEM techniques to positively identify and analyze organelle association in cells expressing endogenous Cx43.

It was determined, based on ultrastructural analysis of the structures in the cytoplasm that some of the puncta identified as annular gap junction at the light microscopic level of resolution could be cytoplasmic aggregates or fragments. It should be noted however that such structures were relatively rare, and thus our findings would be consistent with most of the puncta seen with live cell imaging being annular gap junctions. The average puncta size measured from live cell imaging of Cx43-GFP expressing cells was $1.6 \pm 0.3 \mu\text{m}^2$, a size previously shown to be consistent with annular gap junctions and not secretory vesicles[19,40]. We did not see interactions of cytoplasmic membrane aggregates and fragments with other mitochondria or lysosomes, however this is not to say that it did not occur. We may have missed such interactions due to the limits of seeing three-dimensional occurrences with TEM techniques, especially if the occurrence was rare.

It is well accepted that once internalized, the connexin in annular gap junction vesicles are degraded by lysosomes[7,13,14,24,42-45]. This is based on TEM observations of lysosomes and annular gap junction vesicles fusion[7,14], the increase in annular gap junction vesicles when lysosomal activity is inhibited[44], and the demonstration of acid phosphatase activity in these annular gap junctions[7,13,14]. In this current study we have quantitated annular/lysosome associations, and contrasted this with interactions of annular gap junction vesicles with mitochondria. We found with TEM, that only 2.6 % of the annular gap junction vesicles analyzed were associated with lysosomes at a given point in time. Although this figure may suggest a limited contribution to the process, any alteration in the rate of Cx43 degradation might serve as a post-translational means of altering intercellular communication in some cell types.

The association between mitochondria and annular gap junction vesicles was not expected and it has not been, to our knowledge, previously reported. The contact between mitochondria and annular gap junctions was a distance as close as 10–30nm at the site of contact and in some cases the two membranes of the two organelles were actually in physical contact with one another. This is comparable to the distance of 10–30nm between the mitochondria and ER at their points of contact. The existence of ER-mitochondria contact sites has been well established by electron microscopy and time-lapse fluorescence microscopy and it has been suggested that in Yeast, a network of contact sites serve to integrate the ER, vacuoles, and mitochondria[48]. Here we suggest that in addition to the interaction between ER, and vacuoles that mitochondria also interact with annular gap junction vesicles. The benefit of this interaction can only be speculated at this point but it is tempting to suggest that Cx43 from annular gap junctions may be delivered to mitochondria when the two organelles come into physical contact. It is possible that connexins are delivered to the mitochondria in secretory vesicles, and we have not ruled out that possibility. However, the intimate physical association of the membranes of the mitochondria and annular gap junction would suggest the possibility of Cx43 delivery to the mitochondrial membrane.

Proof of mitochondrial Cx43 have been provided from investigators who used a wide variety of different techniques, including immunocytochemical colocalization of Cx43 with mitochondrial proteins at the light microscopic and immunogold electron microscopic levels of resolution [49], flow cytometry studies, and quantitative Western blot analysis [49,52-54]. Mitochondrial Cx43 has been demonstrated to in protecting the heart from ischemic injury, facilitating mitochondrial movement to the cell periphery as well as maintaining mitochondrial network integrity [37-39, 49-51 54-57]. Further, mitochondrial metabolic activity and morphology alterations have been demonstrated in adipocytes from Cx43 knockout mice and knocked down cells in culture[38], consistent with there being a Cx43 mitochondrial functional dependency[49-51].

The questions of how connexin reaches and incorporates into mitochondria membranes and further its orientation once there (Cx43 C-terminal tail toward the cytoplasm or the inner mitochondrial matrix), and its physical arrangement (single Cx43 molecules or hemichannels) have not been answered. It is known that mitochondrial Cx43 is phosphorylated [56] however it is not known which Cx43 amino acid residuals are phosphorylated. The mechanism that regulates trafficking of Cx43 to the mitochondria and its protective role in pathophysiological conditions remain unknown.

Is the annular gap junction vesicle possible a cytoplasmic source of phosphorylated Cx43 that could potentially serve as a source for distribution Cx43 to other compartments? Although it well accepted that connexins in annular gap junctions are degraded, other possible fates have received little attention despite the reports of Cx43 recycling from annular gap junctions to participate in rapid gap junction plaque formation at the end of the mitotic process [25,26].

The ultrastructural finding that some annular gap junctions, coated with clathrin or with bud-like projections, were found fused to lysosomes was surprising. Normally the clathrin coat disassembles from vesicles after 60-100 seconds and is lost once these vesicles associate with other organelles[46,47]. That the clathrin coat remains with the annular gap junction vesicle, even when that structure is fused with lysosomes, is suggestive of a role of clathrin in annular gap junction processing, including the possible release of buds from the annular gap junction. The release of small buds from annular gap junctions has been demonstrated[41]. It is possible that Cx43 in these “annular gap junction buds” may be degraded but in addition this Cx43 may be delivered in these buds to other organelles, including mitochondria.

The method by which Cx43 traffics to the mitochondria has not been elucidated here. However, the findings of targeting and functional changes in mitochondrial function and movement points to the possibility that in addition to traditional Cx43 trafficking and function at the cell surface that Cx43 may traffic and function in non-canonical manners. Here we demonstrate the association of annular gap junctions with mitochondria and suggest that Cx43 in annular gap junctions may have a fate that is unrelated to degradation. Future studies are needed to elucidate the ‘tethering’ molecules that hold annular gap junctions to mitochondria and to clarify the need for the interaction annular gap junctions with mitochondria.

4. Materials and Methods

4.1 Cell Culture

SW-13 human adrenocortical tumor cells (American Type Culture Collection, Rockville, MD) were cultured in L-15 medium which contained fetal calf serum (10%), penicillin (0.06 mg/ml), streptomycin (0.1 mg/ml), and Fungizone (0.01 mg/ml), buffered with L-arginine at pH 7.4 (reagents and medium from Invitrogen, Carlsbad, CA). Cells were grown at 37°C in a 5% CO₂ atmosphere.

4.2 Gap Junction Antibodies and Probes

Affinity purified polyclonal rabbit antibodies (IgG), were prepared against synthetic peptides corresponding to the carboxyl terminus of the Cx43 molecule (residues 370 to 381) [57] (Zymed Laboratory, San Francisco, CA). Preparation and characterization of these antibodies have been previously described [2].

4.3 Immunocytochemistry

Cells were prepared and stained with immunocytochemical techniques, as previously described [58,59] for connexin 43 (1:100; Proteintech, Rosemont, IL), clathrin (Abcam, Cambridge, MA), lysosomes with Lamp1 staining (Abcam, Cambridge, MA), and mitochondrial proteins either with (mouse monoclonal antibody to prohibitin (1:100 dilution) (NeoMarkers, Fremont, CA), Mitotracker, or Tom20 (Santa Cruz, Dallas, TX). Prior to immunocytochemical procedures, the cells were grown on coverslips, rinsed with phosphate buffered saline solution (PBS), fixed at room temperature, in 3% formaldehyde for 20 minutes, permeabilized in cold acetone for 7 minutes, and then incubated at 37°C for one hour or at 4°C overnight in the primary antibody. In some experiments colocalization studies were performed. In these procedures, labeling of connexin was followed by a 4°C overnight incubation in clathrin antibody. In experiments to colocalize mitochondria, the cellular localization of prohibitin, TOMM-20, or mitotracker was visualized with a fluorescein isothiocyanate conjugated goat anti-mouse secondary antibody (1:1000;

Pierce, Rockford, IL). The coverslips were stained with Hoescht, washed in PBS, and placed onto glass slides with a drop of Fluoromount-G anti-quench reagent (Southern Biotechnical Lab, Birmingham, AL). Immunolabeled cells were imaged at 63X with an Olympus Provis microscope (Olympus, Center Valley, PA).

For immunocytochemical analysis, the number of gap junction plaques and annular vesicles per cell nuclei were calculated. Fluorescent spherical puncta that were greater-or-equal to 0.5 μ m in diameter were classified as annular gap junction vesicles while plaques were identified by their typical elongated profile or by the presence of aggregated puncta (smaller plaques), that were obviously at the cell surface between two cell pairs. The data was expressed as the average number of annular gap junction vesicles per cell.

4.5 Percent Colocalization

The percent colocalization was calculated from 50 cells (10 cells were selected from each of five files) in images collected by confocal step through selecting elements at the mid-plane of the Z stack. All images were saved as tiffs prior to analysis. The MetaMorph Software Program was used to view and trace the cell borders and to determine the percent calculation of cells positive for both signals. Specifically the merged image was separated into red and green channels and the trace areas were then transferred to the separated images. After thresholding the images the number of Cx43 containing objects was determined with the automatic counting tool in MetaMorph. The counts were displayed on the "record count screen", which was then analyzed and the number of surface gap junctions (as well as the number of clusters or aggregates or any object that did not look like an annular gap junction) were counted manually and subtracted from the total number of objects. The number of overlapping areas (yellow objects) were then counted manually by analyzing the merged image. The number of annular gap junctions that colocalized with lysosomes or mitochondria were determined by counting the number of annular gap junctions that had any yellow associated with them. The data was expressed as the average percent colocalization of annular gap junction vesicles with lysosomes or mitochondria.

4.6 Transfection with cDNA

To visualize gap junction trafficking in living cells, adrenal cells were transfected with cDNAs encoding the fluorescent Cx43-GFP (provided by Dr. M. Falk, Lehigh University). The Cx43-GFP vector was constructed by linking the GFP fluorescent reporter protein to the C-terminus of the rat Cx43 cDNA, and it has been demonstrated to assemble into gap junction plaques similar to wild type Cx43 [60]. Lipofectamine²⁰⁰⁰ Transfection Reagent (Life Technologies, Grand Island, NY) was used to establish cell populations that transiently expressed fluorescently tagged Cx43, GFP, or empty vector.

The day before transfection, cells were seeded onto coverslips or in Mattek cell culture dishes (MatTek Corporation, Ashland, MA). Cell populations, at 70-80% confluence, were transfected in Opti-mem medium which contained Lipofectamine²⁰⁰⁰ Transfection Reagent (Invitrogen, Carlsbad, CA) and 4 μ g of plasmid DNA (Cx43-GFP, or empty vector) for 24 hours at 37°C in an atmosphere of 5% CO₂. The resulting complexes were removed by gentle aspiration and washed with PBS. Fresh L-15 complete cell growth medium was added to the dishes, and the cells were incubated at 37°C in 5% CO₂ for 24-48 hours before imaging.

4.7 Imaging of Cx43-GFP in Living Cells

MatTek glass bottom dishes with cells expressing Cx43-GFP or empty vector were placed into a temperature controlled chamber and maintained at 37°C in 5% CO₂ on a live cell Nikon A1 series automatic confocal laser point scanning system (Nikon Instruments Inc., Melville, NY). Image acquisition on the Olympus was performed with a MetaMorph Imaging System (Molecular Devices, Downingtown, PA) and Nikon NIS-Elements on the A1 Nikon microscope.

Images were obtained with a 63x oil objective with a numerical aperture of 1.4. Images were collected at 1-5 minute intervals. DIC and fluorescent images were obtained using the standard fluorescence detector at wavelengths 482 and 595 for all experiments. Focus was maintained with the Perfect Focus System (PFS) function and images were acquired with Nikon's NIS-Elements software. Qualitative and quantitative analyses were performed on the data sets with the rendering tool in NIS-Elements. Time lapse images were used to analyze gap junction plaque internalization in and for analysis, time-lapse movies were converted to movies and evaluated with the MetaMorph program (Molecular Devices, Downingtown, PA).

Annular gap junction vesicle pattern of displacement within the cell and corresponding changes in size (area expressed as μm^2) were quantitated with the tracking function in the Imaris analysis software (Bitplane Scientific, South Windsor, CT). Selected annular vesicles were segmented based upon labeling intensity and then followed over time. Statistical significance of differences was determined with the Student's t-Test.

4.8 Super-resolution-Live Cell Microscopy

Super-resolution microscopy was used to analyze annular gap junction and mitochondrial interaction with the stimulated emission depletion (STED) microscopy technique. STED allows for enhanced spatial resolution of the mitochondria which improves our accuracy when analyzing annular gap junction associations with mitochondria across the x, y, and z planes. Gated STED images were obtained using a commercial Leica SP8 STED 3X system (Leica Microsystems, Mannheim, Germany) housing a 100x oil objective with a numerical aperture of 1.4. Connexin 43 and Tomm-20 antibodies were used to label annular gap junctions and mitochondria, respectively, for STED imaging.

4.9 Transmission Electron Microscopy

Cell monolayers were briefly rinsed in PBS then fixed with 2.5% glutaraldehyde in PBS, pH 7.4, for 1 hour at room temperature. All samples were then washed 3 times in PBS buffer and post-fixed for 1 hour at 4°C in 1% osmium tetroxide with 1% potassium ferricyanide. The samples were washed again and the cells were serially dehydrated in an ethanol (30%, 50%, 70%, and 90%) for 10 minutes and followed by 15 minutes in 100% ethanol three times. The cells were then incubated in Epon 3 times for 1 hour and finally embedded in resin to be sectioned. Ultra-thin sections were cut, mounted on grids, and imaged on a JEOL 1011CX electron microscope (JEOL, Tokyo, Japan).

In Quantum dots protocols and in some protocols to view annular gap junction/organelle contacts, the cells were fixed (2% paraformaldehyde and 0.1% glutaraldehyde in PBS). Quantum dots (QDs) were used to specifically label connexin, and clathrin. Adrenal cells were incubated in Cx43 or clathrin primary antibodies, followed by incubation in biotin IgG conjugated antibody, and then in a QD conjugated secondary antibody (Streptavidin conjugated with QD 655).

Two procedures were used to test the specificity of the quantum dot immuno-electron staining. First, the cells were incubated in the quantum dot-linked anti-rabbit immunoglobulin without a pre-incubation of the thin sections in the first antibody. Second, the binding of quantum dot complexes to embedding resin was evaluated in areas free of cells.

Author Contributions: CLB and SAM conceived, designed and performed the experiments; CLB, TIS, and SAM analyzed the data; CLB, TIS, and SAM wrote the paper.

Funding: This research was funded by National Science Foundation grant #MCB-1408986.

Acknowledgments: We would like to thank the following people at the University of Pittsburgh: Dr. Beth Nickel, Margaret Bisher, Deborah O. Osakue, Dr. Simon Watkins, Dr. Claudette St. Croix, and Michael Caldron. We would like to acknowledge the NIH supported microscopy resources in the University of Pittsburgh Center for Biologic Imaging, specifically, the confocal microscope supported by grant number 1S10OD019973-01. We would also like to thank Dr. Winston Thompson of Morehouse School of Medicine for providing us with prohibitin.

Conflicts of Interest: The authors declare no conflict of interest

Abbreviations

TEM	Transmission Electron Microscopy
QDs	Quantum Dots
AGJ	Annular Gap Junction Vesicle

References

1. Goodenough, D.A.; Goliger, J.A.; Paul, D.L. Connexins, Connexons, and intercellular communication (Review). *Ann Rev Biochem* **1996** *65*, 475-502. <https://doi.org/10.1146/annurev.bi.65.070196.002355>.
2. Kumar, N.M.; Gilula, N.B. Molecular biology and genetics of gap junction channels. *Seminars in Cell Biology* **1992** *3*, 3-16. [https://doi.org/10.1016/S1043-4682\(10\)80003-0](https://doi.org/10.1016/S1043-4682(10)80003-0).
3. Kumar, N.M.; Gilula, N.B. Cloning and characterization of human and rat liver cDNAs coding for a gap junction protein. *J Cell Bio* **1986** *103*, 767-76. <https://doi.org/10.1083/jcb.103.3.767>.
4. Gilula, N.B. Topology of gap junction protein and channel function. *Ciba Foundation Symposium* **1987** *125*, 128-39. [https://doi.org/10.1016/0022-2836\(92\)90253-G](https://doi.org/10.1016/0022-2836(92)90253-G).
5. Ahmad, S.; Diez, J.A.; George, C.H.; Evans, W.H. Synthesis and assembly of connexins in vitro into homomeric and heteromeric functional gap junction hemichannels. *Biochemical Journal* **1999** *339*, 247-53. <https://doi.org/10.1042/0264-6021:3390247>.
6. Perkins, G.A.; Goodenough, D.A.; Sosinsky, G.E. Formation of the gap junction intercellular channel requires a 30 degree rotation for interdigitating two apposing connexons. *Journal of Molecular Biology* **1998** *277*, 171-7. <https://doi.org/10.1006/jmbi.1997.1580>.
7. Murray, S.A.; Larsen, W.J.; Trout, J.; Donta, S.T. Gap junction assembly and endocytosis correlated with patterns of growth in a cultured adrenocortical tumor cell (SW-13). *Cancer Res* **1981** *41*, 4063-74.
8. Falk, M.M.; Bell, C.L.; Kells Andrews, R.M.; Murray, S.A. Molecular mechanisms regulating formation, trafficking and processing of annular gap junctions. *BMC Cell Biology Journal, Section: Cell-Cell Contacts* **2016** *17*, 5-23. <https://doi.org/10.1186/s12860-016-0087-7>.
9. Nickel, B.M.; DeFranco, B.H.; Gay, V.L.; Murray, S.A. Clathrin and Cx43 gap junction plaque endoexocytosis. *Biochem Biophys Res Commun* **2008** *374*, 679-82. <https://doi.org/10.1016/j.bbrc.2008.07.108>.
10. Huang, X.D.; Horackova, M.; Pressler, M.L. Changes in the expression and distribution of connexin 43 in isolated cultured adult guinea pig cardiomyocytes. *Experimental Cell Research* **1996** *228*, 254-61. <https://doi.org/10.1006/excr.1996.0324>.
11. Gumpert, A.M.; Varco, J.S.; Baker, S.M.; Piehl, M.; Falk, M.M. Double-membrane gap junction internalization requires the clathrin-mediated endocytic machinery. *FEBS Lett* **2008** *582*, 2887-92. <https://doi.org/10.1016/j.febslet.2008.07.024>.
12. Piehl, M.; Lehmann, C.; Gumpert, A.; Denizot, J.P.; Segretain, D.; Falk, M.M. Internalization of Large Double-Membrane Intercellular Vesicles by a Clathrin-dependent Endocytic Process. *Mol Biol Cell* **2007** *18*, 337-47. <https://doi.org/10.1091/mbc.E06-06-0487>.

13. Larsen, W.J.; Tung, H.N.; Murray, S.A.; Swenson, C.A. Evidence for the participation of actin microfilaments and bristle coats in the internalization of gap junction membrane. *J Cell Biol* **1979** *83*, 576-87. <https://doi.org/10.1083/jcb.83.3.576>.
14. Larsen, W.J.; Hai, N. Origin and fate of cytoplasmic gap junctional vesicles in rabbit granulosa cells. *Tissue & Cell* **1978** *10*, 585-98. [https://doi.org/10.1016/S0040-8166\(16\)30351-2](https://doi.org/10.1016/S0040-8166(16)30351-2).
15. Jordan, K.; Chodock, R.; Hand, A.R.; Laird, D.W. The origin of annular junctions: a mechanism of gap junction internalization. *J Cell Sci* **2001** *114*, 763-73.
16. Naus, C.C.; Hearn, S.; Zhu, D.; Nicholson, B.J.; Shivers, R.R. Ultrastructural analysis of gap junctions in C6 glioma cells transfected with connexin43 cDNA. *Experimental Cell Research* **1993** *206*, 72-84. <https://doi.org/10.1006/excr.1993.1122>.
17. Dermietzel, R.; Hertberg, E.L.; Kessler, J.A.; Spray, D.C. Gap junctions between cultured astrocytes: immunocytochemical, molecular, and electrophysiological analysis. *Journal of Neuroscience* **1991** *11*, 1421-32. <https://doi.org/10.1523/JNEUROSCI.11-05-01421.1991>.
18. Risley, M.S.; Tan, I.P.; Roy, C.; Saez, J.C. Cell-, age- and stage-dependent distribution of connexin43 gap junctions in testes. *Journal of Cell Science* **1992** *103*, 81-96.
19. Jordan, K.; Solan, J.L.; Dominguez, M.; Sia, M.; Hand, A.; Lampe, P.D.; Laird, D.W. Trafficking, assembly, and function of a connexin43-green fluorescent protein chimera in live mammalian cells. *Mol Biol Cell* **1999** *10*, 2033-50.
20. Segretain, D.; Falk, M.M. Regulation of connexin biosynthesis, assembly, gap junction formation, and removal. *Biochim Biophys Acta* **2004** *1662*, 3-21. <https://doi.org/10.1016/j.bbamem.2004.01.007>.
21. Lauf, U.; Giepmans, B.N.; Lopez, P.; Braconnot, S.; Chen, S.C.; Falk, M.M. Dynamic trafficking and delivery of connexons to the plasma membrane and accretion to gap junctions in living cells. *Proc Natl Acad Sci U S A* **2002** *99*, 10446-51. <https://doi.org/10.1073/pnas.162055899>.
22. Sosinsky, G.E.; Gaietta, G.M.; Hand, G.; Deerinck, T.J.; Han, A.; Mackey, M.; Adams, S.R.; Bouwer, J.; Tsien, R.Y.; Ellisman, M.H. Tetracysteine genetic tags complexed with biarsenical ligands as a tool for investigating gap junction structure and dynamics. *Cell Commun Adhes* **2003** *10*, 181-6. <https://doi.org/10.1080/cac.10.4-6.181.186>.
23. Nickel, B.; Boller, M.; Schneider, K.; Shakespeare, T.; Gay, V.; Murray, S.A. Visualizing the effect of dynamin inhibition on annular gap vesicle formation and fission. *J Cell Sci* **2013** *126 Pt 12*, 2607-16. <https://doi.org/10.1242/jcs.116269>.
24. Qin, H.; Shao, Q.; Igdoura, S.A.; Alaoui-Jamali, M.A.; Laird, D.W. Lysosomal and proteasomal degradation play distinct roles in the life cycle of Cx43 in gap junctional intercellular communication-deficient and -competent breast tumor cells. *J Biol Chem* **2003** *278*, 30005-14. <https://doi.org/10.1101/cshperspect.a002576>.
25. Boassa, D.; Solan, J.L.; Papas, A.; Thornton, P.; Lampe, P.D.; Sosinsky, G.E. Trafficking and recycling of the connexin43 gap junction protein during mitosis. *Traffic* **2010** *11*, 1471-86. <https://doi.org/10.1111/j.1600-0854.2010.01109.x>.
26. Vanderpuye, O.A.; Bell, C.L.; Murray, S.A. Redistribution of connexin 43 during cell division. *Cell Biology International* **2016** *40(4)*, 387-96. <https://doi.org/10.1002/cbin.10576>.
27. Solan, J.L.; Lampe, P.D. Kinase programs spatiotemporally regulate gap junction assembly and disassembly: Effects on wound repair. *Semin Cell Dev Biol* **2016** *50*, 40-8. <https://doi.org/10.1016/j.semcdb.2015.12.010>.
28. Lampe, P.D.; Kistler, J.; Hefti, A.; Bond, J.; Muller, S.; Johnson, R.G.; Engel, A. In vitro assembly of gap junctions. *Journal of Structural Biology* **1991** *107*, 281-90. [https://doi.org/10.1016/1047-8477\(91\)90053-Y](https://doi.org/10.1016/1047-8477(91)90053-Y).
29. Musil, L.S.; Le, A.C.; VanSlyke, J.K.; Roberts, L.M. Regulation of connexin degradation as a mechanism to increase gap junction assembly and function. *Journal of Biological Chemistry* **2000** *275*, 25207-15. <https://doi.org/10.1074/jbc.275.33.25207>.
30. Lampe, P.D.; Lau, A.F. Regulation of gap junctions by phosphorylation of connexins. *Arch Biochem Biophys* **2000** *384*, 205-15. <https://doi.org/10.1006/abbi.2000.2131>.
31. Lo, C.W.; Wessels, A. Cx43 gap junctions in cardiac development. *Trends Cardiovasc Med* **1998** *8*, 264-9. [https://doi.org/10.1016/S1050-1738\(98\)00018-8](https://doi.org/10.1016/S1050-1738(98)00018-8).
32. Loewenstein, W.R.; Rose, B. The cell-cell channel in the control of growth. *Seminars in Cell Biology* **1992** *3*, 59-79. [https://doi.org/10.1016/S1043-4682\(10\)80008-X](https://doi.org/10.1016/S1043-4682(10)80008-X).

33. Defranco, B.H.; Nickel, B.M.; Baty, C.J.; Martinez, J.S.; Gay, V.L.; Sandulache, V.C.; Hackam, D.J.; Murray, S.A. Migrating cells retain gap junction plaque structure and function. *Cell Commun Adhes* **2008** *15*, 273-88. <https://doi.org/10.1080/15419060802198298>.
34. Schulz, R.; Gres, P.; Skyschally, A.; Duschin, A.; Belosjorow, S.; Konietzka, I.; Heusch, G. Ischemic preconditioning preserves connexin 43 phosphorylation during sustained ischemia in pig hearts in vivo. *FASEB J* **2003** *17*, 1355-7. <https://doi.org/10.1096/fj.02-0975fje>.
35. Schulz, R.; Boengler, K.; Totzeck, A.; Luo, Y.; Garcia-Dorado, D.; Heusch, G. Connexin 43 in ischemic pre- and postconditioning. *Heart Fail Rev* **2007** *12*, 261-6. <https://doi.org/10.1007/s10741-007-9032-3>.
36. Yao, J.A.; Hussain, W.; Patel, P.; Peters, N.S.; Boyden, P.A.; Wit, A.L. Remodeling of gap junctional channel function in epicardial border zone of healing canine infarcts. *Circ Res* **2003** *92*, 437-43. <https://doi.org/10.1161/01.RES.0000059301.81035.06>.
37. Fu, Y.; Zhang, S.S.; Xiao, S.; Basheer, W.A.; Baum, R.; Epifantseva, I.; Hong, T.; Shaw, R.M. Cx43 Isoform GJA1-20k Promotes Microtubule Dependent Mitochondrial Transport. *Front Physiol* **2017** *8*, 905. <https://doi.org/10.1080/15419060701402320>.
38. Kim, S.N.; Kwon, H.J.; Im, S.W.; Son, Y.H.; Akindehin, S.; Jung, Y.S.; Lee, S.J.; Rhyu, I.J.; Kim, I.Y.; Seong, J.K.; Lee, J.; Yoo, H.C.; Granneman, J.G.; Lee, Y.H. Connexin 43 is required for the maintenance of mitochondrial integrity in brown adipose tissue. *Sci Rep* **2017** *7*, 7159. <https://doi.org/10.1002/bies.10159>.
39. Boengler, K.M.; Ruiz-Meana, et al. Mitochondrial connexin 43 impacts on respiratory complex I activity and mitochondrial oxygen consumption. *J Cell Mol Med* **2012** *16*: 1649-55. <https://doi.org/10.1111/j.1582-4934.2011.01516>.
40. Evans, W.H.; Martin, P.E. Lighting up gap junction channels in a flash. *Bioessays* **2002** *24*, 876-80. <https://doi.org/10.1159/000092562>.
41. Gilleron, J.; Carette, D.; Fiorini, C.; Dompierre, J.; Macia, E.; Denizot, J.; Segretain, D.; Pointis, G. The large GTPase dynamin2: a new player in connexin 43 gap junction endocytosis, recycling and degradation. *Int J Biochem Cell Biol* **2011** *43*(8):1208-17. <https://doi.org/10.1093/carcin/17.9.1791>.
42. Falk, M.M.; Fong, J.T.; Kells, R.M.; O'Laughlin, M.C.; Kowal, T.J.; Thevenin, A.F. Degradation of endocytosed gap junctions by autophagosomal and endo-/lysosomal pathways: a perspective. *J Membr Biol* **2012** *245*, 465-76. <https://doi.org/10.1007/s00232-012-9461-3>.
43. Salameh, A. Life cycle of connexins: regulation of connexin synthesis and degradation. *Adv Cardiol* **2006** *42*, 57-70. <https://doi.org/10.1038/nsmb.1985>.
44. Guan, X.; Ruch, R.J. Gap junction endocytosis and lysosomal degradation of connexin43-P2 in WB-F344 rat liver epithelial cells treated with DDT and lindane. *Carcinogenesis* **1996** *17*, 1791-8. <https://doi.org/10.1073/pnas.1018845108>.
45. Su, V.; Cochrane, K.; Lau, A.F. Degradation of connexins through the proteasomal, endolysosomal and phagolysosomal pathways. *J Membr Biol* **2012** *245*, 389-400. <https://doi.org/10.1016/j.cardiores.2005.04.014>.
46. Bocking, T.; Aguet, F.; Harrison, S.C.; Kirchhausen, T. Single-molecule analysis of a molecular disassemblase reveals the mechanism of Hsc70-driven clathrin uncoating. *Nat Struct Mol Biol* **2011** *18*, 295-301. <https://doi.org/10.1161/01.RES.0000233145.94073.b8>.
47. Rothnie, A.; Clarke, A.R.; Kuzmic, P.; Cameron, A.; Smith, C.J. A sequential mechanism for clathrin cage disassembly by 70-kDa heat-shock cognate protein (Hsc70) and auxilin. *Proc Natl Acad Sci U S A* **2011** *108*, 6927-32. <https://doi.org/10.1016/j.bbrc.2006.10.177>.
48. van der Blik, A.M.; Shen, Q.; Kawajiri, S. Mechanisms of mitochondrial fission and fusion. *Cold Spring Harb Perspect Biol* **2013** *5*. <https://doi.org/10.1586/14789450.1.3.293>.
49. Boengler, K.; Dodoni, G.; Rodriguez-Sinovas, A.; Cabestrero, A.; Ruiz-Meana, M.; Gres, P.; Konietzka, I.; Lopez-Iglesias, C.; Garcia-Dorado, D.; Di Lisa, F.; Heusch, G.; Schulz, R. Connexin 43 in cardiomyocyte mitochondria and its increase by ischemic preconditioning. *Cardiovasc Res* **2005** *67*, 234-44. [https://doi.org/10.1016/0022-2836\(92\)90253-G](https://doi.org/10.1016/0022-2836(92)90253-G).
50. Halestrap, A.P. Mitochondria and preconditioning: a connexin connection? *Circ Res* **2006** *99*, 10-2. <https://doi.org/10.1161/01.RES.0000233145.94073.b8>.
51. Goubaeva, F.; Mikami, M.; Giardina, S.; Ding, B.; Abe, J.; Yang, J. Cardiac mitochondrial connexin 43 regulates apoptosis. *Biochem Biophys Res Commun* **2007** *352*, 97-103. <https://doi.org/10.1016/j.bbrc.2006.10.177>.
52. Rodriguez-Sinovas, A.; Boengler, K.; Cabestrero, A.; Gres, P.; Morente, M.; Ruiz-Meana, M.; Konietzka, I.; Miro, E.; Totzeck, A.; Heusch, G.; Schulz, R.; Garcia-Dorado, D. Translocation of connexin 43 to the inner

-
- mitochondrial membrane of cardiomyocytes through the heat shock protein 90-dependent TOM pathway and its importance for cardioprotection. *Circ Res* **2006** 99, 93-101.
<https://doi.org/10.1161/01.RES.0000230315.56904.de>.
53. Miro-Casas, E.; Ruiz-Meana, M.; Agullo, E.; Stahlhofen, S.; Rodriguez-Sinovas, A.; Cabestrero, A.; Jorge, I.; Torre, I.; Vazquez, J.; Boengler, K.; Schulz, R.; Heusch, G.; Garcia-Dorado, D. Connexin43 in cardiomyocyte mitochondria contributes to mitochondrial potassium uptake. *Cardiovasc Res* **2009** 83, 747-56. <https://doi.org/10.1093/cvr/cvp157>.
54. Boengler, K.; Konietzka, I.; Buechert, A.; Heinen, Y.; Garcia-Dorado, D.; Heusch, G.; Schulz, R. Loss of ischemic preconditioning's cardioprotection in aged mouse hearts is associated with reduced gap junctional and mitochondrial levels of connexin 43. *Am J Physiol Heart Circ Physiol* **2007** 292, H1764-9. <https://doi.org/10.1152/ajpheart.01071.2006>.
55. Rodriguez-Sinovas, A.; Ruiz-Meana, M.; Denuc, A.; Garcia-Dorado, D. Mitochondrial Cx43, an important component of cardiac preconditioning. *Biochim Biophys Acta* **2018** 1860, 174-181. <https://doi.org/10.1016/j.bbamem.2017.06.011>.
56. Ruiz-Meana, M.; Rodriguez-Sinovas, A.; Cabestrero, A.; Boengler, K.; Heusch, G.; Garcia-Dorado, D. Mitochondrial connexin43 as a new player in the pathophysiology of myocardial ischaemia-reperfusion injury. *Cardiovasc Res* **2008** 77, 325-33. <https://doi.org/10.1093/cvr/cvm062>.
57. Yeager, M.; Gilula, N.B. Membrane topology and quaternary structure of cardiac gap junction ion channels. *Journal of Molecular Biology* **1992** 223, 929-48. [https://doi.org/10.1016/0022-2836\(92\)90253-G](https://doi.org/10.1016/0022-2836(92)90253-G).
58. Oyoyo, U.A.; Shah, U.S.; Murray, S.A. The role of alpha1 (connexin-43) gap junction expression in adrenal cortical cell function. *Endocrinology* **1997** 138, 5385-97. <https://doi.org/10.1210/endo.138.12.5617>.
59. Murray, S.A.; Shakespeare, T.I. (2016) Immunofluorescence: application for analysis of connexin distribution and trafficking., pp. 1-19, CRC Press, Taylor & Francis Group, Boca Raton, FL.
60. Falk, M.M. Connexin-specific distribution within gap junctions revealed in living cells. *J Cell Sci* **2000** 113, 4109-20.